

SYNTHESIS, CHARACTERIZATION AND COMPUTATIONAL STUDIES OF (E)-2-[(2-AMINOPYRIDIN-3-YL)IMINO]-METHYL}-4,6-DI-TERT-BUTYLPHENOL

Alexander Carreño^a, Andrés Vega^{a,†}, Ximena Zarate^b, Eduardo Schott^b, Manuel Gacitúa^c, Ninnette Valenzuela^c, Marcelo Preite^d, Juan M. Manríquez^c and Ivonne Chávez^{c,*}^aDepartamento de Ciencias Químicas, Facultad de Ciencias Exactas, Universidad Andrés Bello, República 275, Santiago, Chile^bLaboratorio de Bionanotecnología, Departamento de Ciencias Químico-Biológicas, Universidad Bernardo O'Higgins, General Gana 1780, Santiago, Chile^cDepartamento de Química Inorgánica, Facultad de Química, Pontificia Universidad Católica de Chile, Avenida Vicuña Mackenna 4860, Santiago, Chile^dDepartamento de Química Orgánica, Facultad de Química, Pontificia Universidad Católica de Chile, Avenida Vicuña Mackenna 4860, Santiago, Chile

Recebido em 04/06/2013; aceito em 09/12/2013; publicado na web em 10/04/2014

(E)-2-[(2-Aminopyridin-3-yl)imino]-methyl}-4,6-di-tert-butyl-phenol (**3**), a ligand containing an intramolecular hydrogen bond, was prepared according to a previous literature report, with modifications, and was characterized by UV-vis, FTIR, ¹H-NMR, ¹³C-NMR, HHCOASY, TOCSY and cyclic voltammetry. Computational analyses at the level of DFT and TD-DFT were performed to study its electronic and molecular structures. The results of these analyses elucidated the behaviors of the UV-vis and electrochemical data. Analysis of the transitions in the computed spectrum showed that the most important band is primarily composed of a HOMO→LUMO transition, designated as an intraligand (IL) charge transfer.

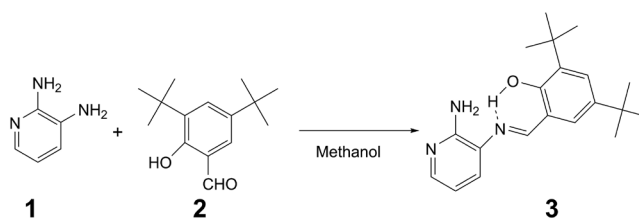
Keywords: intramolecular hydrogen bond; Schiff base; DFT.

INTRODUCTION

Schiff base ligands derived from salicylaldehyde containing OH...N type hydrogen bonding have been studied due to the versatility of their electronic and steric properties.¹⁻³ Different metal complexes with Schiff base ligands have been synthesized and studied because of their ability to form stable complexes.⁴ These complexes have also been used in analytical chemistry for the spectrophotometric determination of heavy metals.^{5,6} Furthermore, they are used as catalysts in chemical and photochemical reactions as well as many other applications. Schiff bases with an -OH group in the *ortho* position relative to an imino group -C=N- have generated much interest due to the existence of an intramolecular hydrogen bond between the OH and the nitrogen atom.^{7,8} Bio-inspired compounds that contain an intramolecular hydrogen bond have been utilized as dyes in photoelectrochemical cells.⁹⁻¹¹ A detailed study of such compounds demonstrated that their electrochemical activity is similar to the activity observed for redox processes in biological systems.¹² This research emphasizes the importance of an intramolecular hydrogen bond in such systems, which has been the subject of much investigation.

With this in mind, we aimed to investigate the possible use of an aminopyridine, (E)-2-[(2-aminopyridin-3-yl)imino]-methyl}-4,6-di-tert-butyl-phenol (**3**, Scheme 1), containing a Schiff base and possessing an intramolecular hydrogen bond as a substituent group. A complete study of its electronic properties was performed to understand the role of the hydrogen bond.

The synthesis and characterization of compound **3** is reported. Compound **3** was obtained from a modified template pathway (Scheme 1), based on a synthesis described by Kleij *et al.*^{13,14} A study of its electronic properties and a computational study were performed, to understand its molecular properties.



Scheme 1. General reaction scheme of (E)-2-[(2-aminopyridin-3-yl)imino]-methyl}-4,6-di-tert-butyl-phenol (compound **3**) synthesis

EXPERIMENTAL

General procedures

NMR spectra were recorded on a Bruker AVANCE 400 MHz NMR spectrometer at 25°C. Samples were dissolved in deuterated chloroform and acetone, using tetramethylsilane as an internal reference. The NMR spectra were processed with TOPSPIN 2.1 program. IR spectra of all compounds were recorded on a Perkin-Elmer 1310 Bruker FT-IR spectrophotometer in KBr discs and were recorded in the range of 250-4000 cm⁻¹. UV-vis spectra were performed using a UV-vis-NIR scanning spectrophotometer Shimadzu Model UV-3101 PC.

For the electrochemical experiments, the working solution contained 9.81 x 10⁻³ mol L⁻¹ of compound **3** with 0.1 mol L⁻¹ tetrabutylammoniumhexafluorophosphate (used as a supporting electrolyte, 99% Aldrich) and TBAPF₆ in CH₃CN (solvent, p.a. Aldrich). Before each experiment, the solution was purged with high purity argon, and an argon atmosphere was maintained over the solution during the entire experiment. A polycrystalline non-annealed platinum disc (diameter 2 mm) was used as the working electrode. Platinum gauze, separated from the cell main compartment by a piece of fine sintered glass, was used as the counter electrode. All potentials in this paper

*e-mail: ichavez@uc.cl

[†]Centro para el Desarrollo de la Nanociencia y la Nanotecnología, CEDENNA

utilize an Ag/AgCl electrode in tetramethylammonium chloride as a reference to match the potential of a saturated calomel electrode (SCE) at room temperature. All electrochemical experiments were performed at room temperature on a CHI900B bipotentiostat interfaced with a PC running CHI 9.12 software for experimental control and data acquisition.

Theoretical computations were performed using density functional theory (DFT) with the B3LYP hybrid exchange/correlation (XC) functional, which includes the non-local exchange term, with three parameters of Becke and the correlation term of Lee-Yang-Parr.^{15,16} Gaussian basis set 6-311+G (2d,p) was employed.¹⁷ Vibrational frequencies were calculated to verify that the stationary state corresponds to a minimum value. Geometric optimizations for the compound were performed. Polarizable continuum model (PCM) was used to simulate the solvent effect using dichloromethane as solvent.^{18–20} In this model, the solvent is characterized for its dielectric constant as well as other parameters. All calculations were made using Gaussian 03.²¹

Syntheses

(E)-2-[[2-(Aminopyridin-3-yl)imino]-methyl]-4,6-di-tert-butylphenol (**3**) was prepared by condensation of 1,2-diaminopyridine (**1**) with 3,5-di-tert-butyl-2-ol-benzaldehyde (**2**) in 20 mL of methanol (see Scheme 1). The reaction was stirred for 24 h at room temperature and then filtered, and the precipitate was washed with methanol and diethyl ether. The yellow product was purified by crystallization, and the product was dried under vacuum. Yellow crystals suitable for X-Ray diffraction were obtained by slow evaporation of the solvent. Yield 70%. UV/VIS: (dichloromethane, $c=4.21 \times 10^{-5}$ mol L⁻¹) λ (ϵ) = 238 (33939.73 mol⁻¹ dm³ cm⁻¹), 279 (23569.23 mol⁻¹ dm³ cm⁻¹), 374 (22419.68 mol⁻¹ dm³ cm⁻¹). (Ethanol, $c=4.21 \times 10^{-5}$ mol L⁻¹) λ (ϵ) = 204 (53751.39 mol⁻¹ dm³ cm⁻¹), 237 (20556.46 mol⁻¹ dm³ cm⁻¹), 373 (12925.49 mol⁻¹ dm³ cm⁻¹). (Acetonitrile, $c=4.21 \times 10^{-5}$ mol L⁻¹) λ (ϵ) = 196 (75455.99 mol⁻¹ dm³ cm⁻¹), 236 (21702.93 mol⁻¹ dm³ cm⁻¹), 370 (12978.52 mol⁻¹ dm³ cm⁻¹).

FTIR (KBr, cm⁻¹): ν_{OH} 3469, ν_{NH_2} 3264 and 3136, $\nu_{\text{C=N}}$ 1609, $\nu_{\text{C=C}}$ 1590. ¹H-NMR (400 MHz, CDCl₃, ppm): δ = 1.28 [s; 9H; -C(CH₃)₃], 1.47 [s; 9H; -C(CH₃)₃], 4.80 [bs; 2H; -NH₂], 6.72 [dd: J=7.6; 5.0 Hz; 1H; H2], 7.24 [m; 1H; H3], 7.26 [d: J=2.0 Hz; 1H; H5], 7.48 [d: J=2.0 Hz; 1H; H6], 8.01 [dd: J=5.0; 1.6 Hz; 1H; H1], 8.63 [s; 1H; H4], 13.03 [s; 1H; OH]. ¹H-NMR (400 MHz, Acetone-d₆, ppm): δ = 1.37 [s; 9H; -C(CH₃)₃], 1.48 [s; 9H; -C(CH₃)₃], 5.48 [bs; 2H; -NH₂], 6.70 [dd: J=7.6; 5.0 Hz; 1H; H2], 7.48 [dd: J=7.6; 1.5 Hz; 1H; H3], 7.49 [d: J=2.5 Hz; 1H; H5], 7.54 [d: J=2.0 Hz; 1H; H6], 7.95 [dd: J=4.9; 1.5 Hz; 1H; H1], 8.88 [s; 1H; H4], 13.30 [s; OH]. ¹³C-NMR (400 MHz, CDCl₃, ppm): δ = 29.42 (-C(CH₃)₃), 31.44 (-C(CH₃)₃), 34.22 (-C(CH₃)₃), 35.13 (-C(CH₃)₃), 114.39 (C10), 118.40 (C11), 124.95 (C12), 126.96 (C4), 128.62 (C5), 130.71 (C9), 137.15 (C7), 141.08 (C1), 146.39 (C3), 153.32 (C2), 157.98 (C8), 164.91 (C6). Anal. Calcd for C₂₀H₂₇N₃O: C, 73.84; H, 8.32; N, 12.92. Found C, 73.74; H, 11.93; N, 13.16.

RESULTS AND DISCUSSION

Compound **3** was a yellow solid obtained in 70% yield. The compound was characterized by FT-IR, and the spectrum exhibits several bands in the range from 2500–4000 cm⁻¹ (Figure 1S in the Supplementary Material). The main absorption frequencies show strong symmetric and asymmetric bands due to an O-H band at 3469 cm⁻¹ and two -NH₂ bands at 3264 and 3136 cm⁻¹. The absorptions near 1609 and 1590 cm⁻¹ were assigned to the stretching of the $\nu_{\text{C=N}}$ and $\nu_{\text{C=C}}$ bonds, respectively, and have been previously reported for a similar compound.^{22,23}

1D and 2D NMR spectra were obtained in CD₃Cl or acetone-d₆ solutions, and the numbering of protons and carbons are provided in the Supplementary Material (Figure 2S and 3S). The ¹HNMR spectrum (CDCl₃, Figures 4S–8S in the S.M.) exhibits a strong peak at approximately 13.03 ppm for -OH, and the amino proton at 4.80 ppm has been previously reported for similar compounds.^{24,25} After D₂O exchange, (Figure 9S in the S.M.) these two signals disappear from the spectrum. Signals assigned to the tert-butyl group appear at 1.47 and 1.28 ppm, and the aromatic protons of both rings appear at 7.50–6.70 ppm and 8.65–8.00 ppm (Figure 10S in the S.M.).

In the pyridine ring, H2 appears at 6.72 ppm, H3 at 7.24 ppm and H1 at 8.01 ppm, while H5 appears at 7.26 ppm and H6 at 7.48 ppm, as shown in Figure 1.

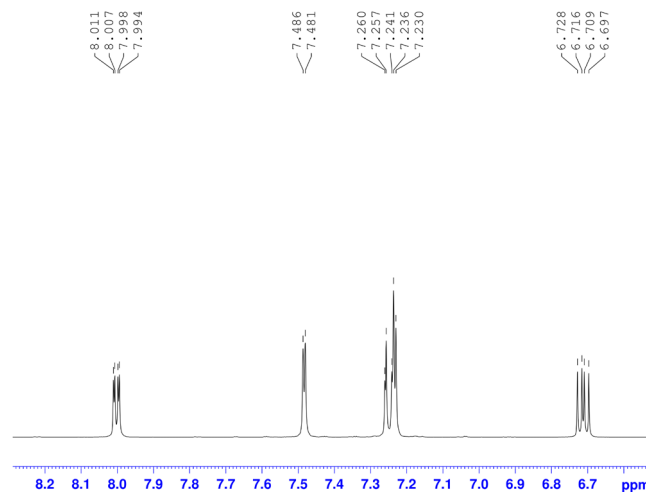


Figure 1. Expanded aromatic region of the ¹HNMR of **3** in CD₃Cl

For the assignment of H3 and H5, which appear between 7.10–7.60 ppm and overlap with the CD₃Cl signal, a spectrum in acetone-d₆ was obtained (Figure 11S in the S.M.). The protons of the pyridine ring appear at 7.95 ppm (H1), 6.70 ppm (H2) and 7.48 ppm (H3), and the signals in the phenol ring appear at 7.49 ppm (H5) and 7.54 ppm (H6) (Figure 12S in the S.M.). To complete the assignment, a 1D TOCSY spectrum allowed us to identify the resonances for all protons (Figure 2). When irradiating at H1 (Figure 2A), an enhancement was observed for H2 and H3. In the same manner, when H2 (Figure 2D) was irradiated, a spectrum showing enhancement for H1 and H2 was obtained. When H5 was irradiated instead (Figure 2B), enhancements in H6, and both -C(CH₃)₃ signals were observed. When H6 was irradiated (Figure 2C), it was impossible to avoid irradiating H3 as well, so enhancements for the H4, H1, H5, H6, H3, H2 and -C(CH₃)₃ signals were observed. These experiments allowed us to assign all signals to their respective protons.

¹³CNMR broad-band decoupled and DEPT spectra in CDCl₃ solution allowed for total peak assignment (Figure 13S and 14S in the S.M.). A signal commonly assigned to the Schiff base carbon (C6) was observed at 169.91 ppm, consistent with previous literature reports.^{4,6} Other signals corresponding to the phenol ring appeared at 157.98 (C8) ppm, and those for the pyridine ring at 153.32 (C2) ppm and 141.08 (C1) ppm.

A crystal structure of compound **3** has been previously reported by Carreño *et al.*, showing an intramolecular hydrogen bond with an OH...N distance of 2.621 Å. The dihedral angle between the aromatic rings is 33°, which is almost planar.²⁶ According to the optimized calculated geometry shown in Figure 3, the molecule adopts a coplanar conformation with an angle between the rings of 39°. Table 1

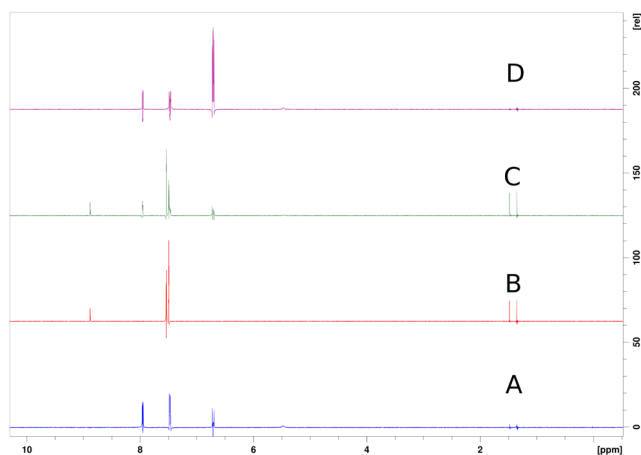


Figure 2. 1D TOCSY experiment for **3** in acetone- d_6 , irradiating at 3182.67 Hz (A), 3014.60 Hz (B), 2998.01 Hz (C) and 2684.80 Hz (D)

Table 1. Selected bond lengths (Å) and angles (°) for compound **3**

	Calculated	Experimental*
C15-N1	1.288	1.279
C3-O1	1.349	1.356
C17-N1	1.406	1.417
C16-N3	1.372	1.357
N1-O-H1A	150.1	149
O1-H1A	0.990	0.840
N1-H1A	1.709	1.870
C15-N1-C17	121.1	119.76

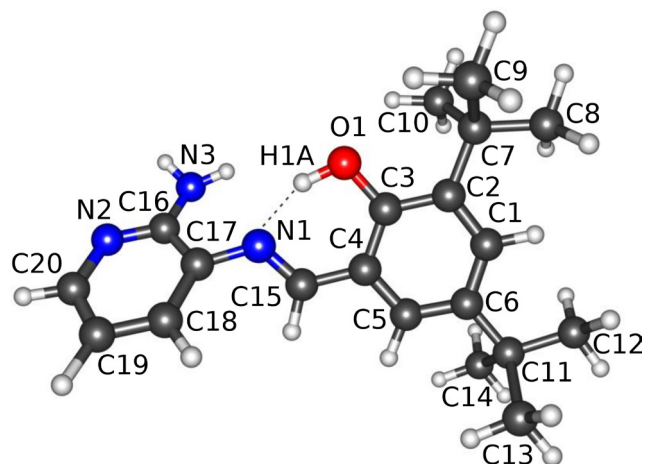


Figure 3. DFT optimized structure of compound **3**

presents the important parameters of the experimental and theoretical data, which agree well.

The UV-vis spectra in dichloromethane, ethanol and acetonitrile showed absorption bands centered at 375 nm and 190 nm (see Table 2), which were assigned to $n \rightarrow \pi^*$ (C=N) and $\pi \rightarrow \pi^*$ transitions.^{27,28} Time-dependent density functional theory (TD-DFT) calculations were conducted further elucidate the UV-vis observed transitions. Figure 4 shows an overlay of the calculated and experimental UV-vis spectra. The composition of the calculated transitions is shown in Table 3. The TD-DFT calculation shows that the absorption band located experimentally at 238 nm ($33939.73 \text{ mol}^{-1} \text{ dm}^3 \text{ cm}^{-1}$) is theoretically found at 233 nm. This calculated transition is composed of a

HOMO \rightarrow LUMO+3 and a HOMO \rightarrow LUMO+4 transition. The bands located experimentally at 281 nm ($23569.23 \text{ mol}^{-1} \text{ dm}^3 \text{ cm}^{-1}$) and at 374 nm ($22419.68 \text{ mol}^{-1} \text{ dm}^3 \text{ cm}^{-1}$) are theoretically calculated at 281 nm and 385 nm, respectively. Those calculated excitations are associated with a HOMO \rightarrow LUMO+1 and a HOMO \rightarrow LUMO transition, respectively. Experimentally, there is no signal shift in the UV-Vis spectra when the solvent polarity changes.

To gain additional insight into the nature of the O-H-N hydrogen bond, topological analysis was performed with the DGrid package in the framework of the atoms in molecules (AIM) theory, which were performed for B3LYP/BAE densities.^{29,30} In this system, a bond critical point (BCP) was found between the H and N atoms and shows a charge density value of 0.0526 a.u., which is the order of magnitude of the charge density in the hydrogen bonds.³¹ In addition, as natural bond orbital (NBO) theory³² studies the role of orbital interactions by considering the interactions between occupied donor and empty acceptor orbitals, the second-order perturbative energy analysis estimates of donor-acceptor interactions in the natural bond orbital (NBO) basis showed an orbital occupancy donated by the nitrogen LP (lone pair) to the BD^* of the hydrogen. This interaction stabilizes the system by $40.28 \text{ kcal mol}^{-1}$.

Table 2. Principal absorption bands of compound **3** in dichloromethane, ethanol and acetonitrile, with λ in nm and ϵ (in $\text{mol}^{-1} \text{ dm}^3 \text{ cm}^{-1}$) in parentheses.

Solvents	$\lambda(\epsilon)$	$\lambda(\epsilon)$	$\lambda(\epsilon)$
Dichloromethane	238 (33939.73)	279 (23569.23)	374 (22419.68)
Ethanol	204 (53751.39)	237 (20556.46)	373 (12925.49)
Acetonitrile	196 (75455.99)	236 (20556.46)	370 (12978.52)

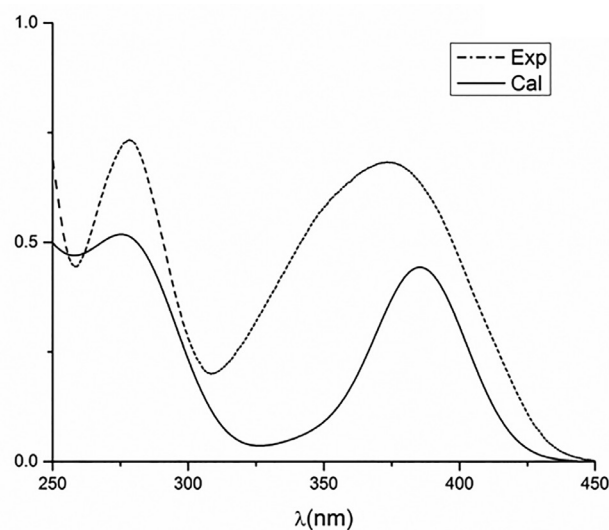


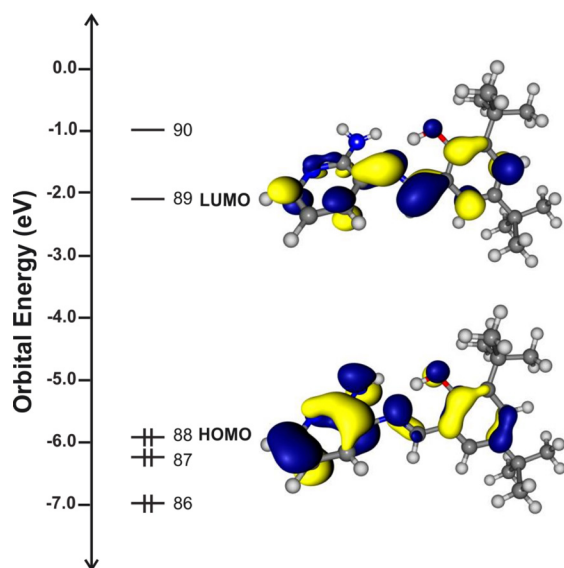
Figure 4. Experimental (---) and calculated (—) (B3LYP/6-311+G(2d,p)) UV-Vis absorption spectra for compound **3**, using dichloromethane as the solvent

Compound **3** exhibits no luminescent properties. Compounds with an imine $\text{N}=\text{CH}$ - bond have been previously reported as not showing emission properties.²³⁻³⁶

The frontier molecular orbitals for compound **3** are plotted in Figure 5. The HOMO is composed mainly of amino and phenol groups, which indicates that these groups are involved in the oxidation process.³⁷ The LUMO is composed of the imine group, which is the region that the electron will be attracted to in the reduction process. The isosurfaces provide some suggestions regarding the experimental results obtained from electrochemical studies.³⁸ The observed behavior agrees with the electrochemical properties shown

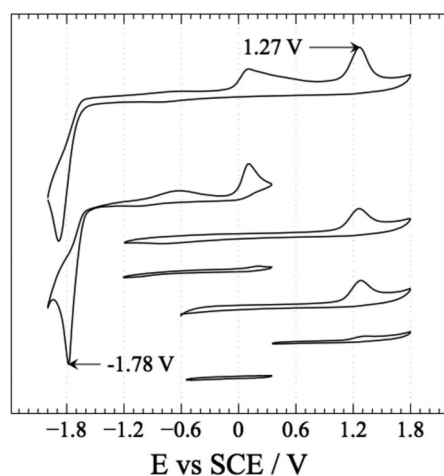
Table 3. Calculated and experimental transitions of compound **3** in dichloromethane

Calculation			Experimental	
λ	Oscillator Strength	Assignment	λ	Extinction coefficient
(nm)	(eV)		(nm)	($\text{mol}^{-1} \text{ dm}^3 \text{ cm}^{-1}$)
233	0.1505	HOMO \rightarrow LUMO+3 HOMO \rightarrow LUMO+4	238	33939.73
281	0.2680	HOMO \rightarrow LUMO+1	279	23569.23
385	0.4403	HOMO \rightarrow LUMO	374	22419.68

**Figure 5.** Energy level diagram of the frontier molecular orbitals for compound **3**

for aminophenol compounds reported by Salavagione *et al.*³⁹

When the electrochemical study was performed with compound **3**, the CV profiles at 200 mV s^{-1} showed several signals (see Figure 6), which were solved by working in the window potential. Compound **3** showed no electrochemical reversible peak potentials, whereas an important irreversible oxidation and an irreversible reduction process were observed.

**Figure 6.** CV profiles of compound **3** at 200 mVs^{-1} . Interface: Pt/ $1.0 \times 10^{-5} \text{ mol L}^{-1}$, $1.0 \times 10^{-4} \text{ mol L}^{-1}$ TBAPF₆ in anhydrous CH₃CN under an argon atmosphere

The voltammetric pattern of compound **3** shows a peak at -1.78 V , which is attributed to the reduction process. This value corresponds

to an irreversible electron transfer.⁴⁰ The irreversible reduction peak is attributed to an intramolecular reductive coupling of the imine group, which involves a self-protonation reaction. In those reactions, the phenolic hydroxyl group acts as a proton donor, and its reductive value depends on the solvent used and on the structure of the Schiff base.⁴¹ Furthermore, one peak is observed at 1.27 V , which is attributed to the oxidation of the NH₂ and OH groups.⁴²⁻⁴⁶

CONCLUSIONS

We synthesized and fully characterized a pyridine Schiff base ligand and showed the presence of an intramolecular hydrogen bond. UV-vis spectra in different solvents showed no band-shift, confirming the stability of the hydrogen bond.

Theoretical geometrical parameters showed good agreement with previously reported experimental data. Additionally, the UV-vis bands were predicted by means of TD-DFT calculations. The stability of the hydrogen bond was also confirmed by the absorption bands, as the first band is located experimentally at 374 nm . Theoretically, this band is centered at 385 nm and is associated with a HOMO LUMO transition with OH group involvement; this transition is described as an intraligand charge transfer.

The voltammetric peak at -1.78 V is attributed to the reduction of the imine group, and involves a self-protonation reaction, as shown previously. This result is consistent with the theoretical study, which shows the importance of the intramolecular hydrogen bond. Additionally, a peak at 1.27 V is observed and attributed to the oxidation of amino and hydroxyl groups. The use of compound **3** as a ligand in d-transition metal complexes will be the subject of further research.

SUPPLEMENTARY MATERIAL

Available at <http://quimicanova.s bq.org.br>, in the form of a PDF file, with free access. The following data, is found: FTIR spectrum (Figure 1S), numbering used in proton and carbon assignments (Figure 2S and 3S), ¹HNMR spectra and aromatic expanded regions in CD₃Cl (Figure 4S to 8S), D₂O exchanged ¹HNMR spectra, in CD₃Cl (Figure 9S), HHCOSY spectra in CD₃Cl (Figure 10S), ¹HNMR spectra and aromatic expanded region, in acetone-d₆ (Figure 11S and 12S), ¹³CNMR and DEPT spectra, in CD₃Cl (Figure 13S and 14S).

ACKNOWLEDGMENT

We are grateful to Dr. Maria A. del Valle (PUC) for access to her instrumental facilities, Dr. Claudio Lopez A. (PUC) for the NMR spectra, and B.A. Alfonso Inzunza G. for his help with the English translation. We thank "Proyecto RC120001 de la Iniciativa Científica Milenio del Ministerio de Economía, Fomento y Turismo" and UNAB-DI-28-10/I for financial support. A. Carreño acknowledges Universidad Andrés Bello for his doctoral fellowship. A. Vega

is a member of “Financiamiento Basal para Centros Científicos y Tecnológicos de Excelencia FB0807”. E. Schott thanks Fondecyt 1130707.

REFERENCES

1. Costamagna, J.; Vargas, J.; Latorre, R.; Alvarado, A.; Mena, G.; *Coord. Chem. Rev.* **1992**, *119*, 67.
2. Gupta, K.C.; Sutar, A.K.; *Coord. Chem. Rev.* **2008**, *252*, 1420.
3. Prakash, A.; Adhikari, D.; *Int. J. Chem.* **2011**, *3*, 1891.
4. Holbach, M.; Zheng, X.; Burd, C.; Jones, C.W.; Weck, M.; *J. Org. Chem.* **2006**, *71*, 2903.
5. Kormaly, E.; Kylic, E.; *Talanta* **2002**, *58*, 793.
6. Fakhari, A.R.; Khorrami, A.R.; Naeimi, H.; *Talanta* **2005**, *66*, 813.
7. Benisvy, L.; Blake, A.J.; Collison, D.; Davies, E.S.; Garner, D.; McInnes, E.J.L.; McMaster, J.; Whittaker, G.; Wilson, C.; *Chem. Commun.* **2001**, 1824.
8. Benisvy, L.; Bill, E.; Blake, A.J.; Collison, D.; Davies, E.S.; Garner, C.D.; Guindy, Ch. I.; McInnes, E.J.L.; McArdle, G.; McMaster, J.; Wilson, C.; Wolowska, J.; *Dalton Trans.* **2004**, 3647.
9. Kodis, G.; Terazono, Y.; Liddell, P.; Andreasson, J.; Garg, V.; Hambourger, M.; Moore, T.; Moore, A.; Gust, D.; *J. Am. Chem. Soc.* **2006**, *128*, 1818.
10. Brune, A.; Jeong, G.; Liddell, P.A.; Sotomura, T.; Moore, T.A.; Moore, A.L.; Gust, D.; *Langmuir* **2004**, *20*, 8366.
11. Moore, G.F.; Hambourger, M.; Gervaldo, M.; Poluektov, O.G.; Rajh, T.; Gust, D.; Moore, T.A.; Moore, A.L.; *J. Am. Chem. Soc.* **2008**, *130*, 10466.
12. Markle, T.F.; Rhile, I.J.; DiPasquale, A.G.; Mayer, J.M.; *PNAS* **2008**, *15*, 8185.
13. Kleij, A.W.; Kuil, M.; Tooke, D.M.; Lutz, M.; Spek, A.L.; Reek, J.N.H.; *Chem. Eur. J.* **2005**, *11*, 4743.
14. Haak, R.M.; Wezenberg, S.J.; Kleij, A.W.; *Chem. Commun.* **2010**, *46*, 2713.
15. Becke, A.D.; *J. Chem. Phys.* **1993**, *98*, 5648.
16. Lee, C.; Yang, W.; Parr, R.G.; *Phys. Rev.* **1998**, *B37*, 785.
17. Ditchfield, R.; Hehre, W.J.; Pople, J.A.; *J. Chem. Phys.* **1971**, *54*, 724.
18. Cossi, M.; Scalmani, G.; Rega, N.; Barone, V.; *J. Chem. Phys.* **2002**, *117*, 43.
19. Cammi, R.; Mennucci, B.; Tomasi, J.; *J. Phys. Chem. A* **2000**, *104*, 5631.
20. Cossi, M.; Barone, V.; *J. Chem. Phys.* **2001**, *115*, 4708.
21. Frisch, M.J.; Trucks, G.W.; Schlegel, H.B.; Scuseria, G.E.; Robb, M.A.; Cheeseman, J.R.; Montgomery, J.A.; Vreven, T.; Kudin, K.N.; Burant, J.C.; Millam, J.M.; Iyengar, S.S.; Tomasi, J.; Barone, V.; Mennucci, B.; Cossi, M.; Scalmani, G.; Rega, N.; Petersson, G.A.; Nakatsuji, H.; Hada, M.; Ehara, M.; Toyota, K.; Fukuda, R.; Hasegawa, J.; Ishida, M.; Nakajima, T.; Honda, Y.; Kitao, O.; Nakai, H.; Klene, M.; Li, X.; Knox, J.E.; Hratchian, H.P.; Cross, J.B.; Adamo, C.; Jaramillo, J.; Gomperts, R.; Stratmann, R.E.; Yazyev, O.; Austin, A.J.; Cammi, R.; Pomelli, C.; Ochterski, J.W.; Ayala, P.Y.; Morokuma, K.; Voth, G.A.; Salvador, P.; Dannenberg, J.J.; Zakrzewski, V.G.; Dapprich, S.; Daniels, A.D.; Strain, M.C.; Farkas, O.; Malick, D.K.; Rabuck, A.D.; Raghavachari, K.; Fores-
- man, J.B.; Ortiz, J.V.; Cui, Q.; Baboul, A.G.; Clifford, S.; Cioslowski, J.; Stefanov, B.B.; Liu, G.; Liashenko, A.; Piskorz, P.; Komaromi, I.; Martin, R.L.; Fox, D.J.; Keith, T.; Al-Laham, M.A.; Peng, C.Y.; Nanayakkara, A.; Challacombe, M.; Gill, P.M.W.; Johnson, B.; Chen, W.; Wong, M.W.; Gonzalez, C.; Pople, J.A.; *Gaussian 03; Computer Program for Computational Chemistry*; Gaussian, Inc.; Pittsburgh, USA, 2003.
22. Ambroziak, K.; Rozwadowski, Z.; Dziembowska, T.; Bieg, B.; *J. Mol. Struct.* **2002**, *615*, 109.
23. Majerz, I.; Pawlukoje, A.; Sobczyk, L.; Dziembowska, T.; Grech, E.; Szady-Chelminiecka, A.; *J. Mol. Struct.* **2000**, *552*, 243.
24. Waldeck, D.H.; *Chem. Rev.* **1991**, 415.
25. Yildiz, M.; Kilic, Z.; Hokelek, T.; *J. Mol. Struct.* **1998**, *441*, 1.
26. Carreño, A.; Ladeira, S.; Castel, A.; Vega, A.; Chávez, I.; *Acta Crystallogr.* **2012**, E68, o2507.
27. Tozzo, E.; Romera, S.; dos Santos, M.P.; Muraro, M.; Santos, R.H.; Liao, L.M.; Vizotto, L.; Dockal, E.R.; *J. Mol. Struct.* **2008**, *876*, 110.
28. Brescian-Pahor, N.; Calligaris, M.; Delise, P.; Dodie, G.; Nardin, G.; Randaccio, L.; *J. Chem. Soc., Dalton Trans.* **1976**, *23*, 2478.
29. Kohout, M.; Programm DGrid; version 4.6; Radebeul, Germany, 2010.
30. Bader, R.F.W. In *Atoms in Molecules: A Quantum Theory*; Bader, R.F.W., eds.; Clarendon Press: Oxford, UK, 1990.
31. Koch, U.; Popelier, P.L.A.; *J. Phys. Chem.* **1995**, *99*, 9747.
32. Foster, J.P.; Weinhold, F.; *J. Am. Chem. Soc.* **1980**, *102*, 7211.
33. Rau, H.; Luddecke, E.; *J. Am. Chem. Soc.* **1982**, *104*, 1616.
34. Karatsu, T.; Kitamura, A.; Zeng, H.; Arai, T.; Sakuragi, H.; Tokumura, K.; *Bull. Chem. Soc. Jpn.* **1995**, *68*, 920.
35. Gopal, R.V.; Reddy, A.M.; Rao, V.J.; *J. Org. Chem.* **1995**, *60*, 7966.
36. Boere, R.T.; Roemmele, T.L.; *Coord. Chem. Rev.* **2000**, *210*, 369.
37. Carreño A.; Gacitúa M.; Linares C.; McLeod Carey D.; Pizarro N.; Preite M.; Manríquez J.M.; Arratia-Perez R.; Vega A.; Chávez I.; *Resumos do XVI Simpósio Brasileiro de Química Teórica*, Ouro Preto, Brasil, 2011.
38. Korth, H.G.; de Heer, M.I.; Mulder, P.; *J. Phys. Chem. A* **2002**, *106*, 8779.
39. Salavagione, H.J.; Arias, J.; Garces, P.; Morallon, E.; Barbero, C.; Vazquez, J.L.; *J. Electroanal. Chem.* **2004**, *565*, 375.
40. Isse, A.; Gennaro, A.; Vianello, E.; *Electrochim. Acta* **1997**, *42*, 13.
41. Zolezzi, S.; Spodine, E.; Decinti, A.; *Polyhedron* **2002**, *21*, 55.
42. Yamada, K.; Teshima, K.; Kobayashi, N.; Hirohashi, R.; *J. Electroanal. Chem.* **1995**, *394*, 71.
43. Lapuente, R.; Cases, F.; Garces, P.; Morallon, E.; Vazquez, J.L.; *J. Electroanal. Chem.* **1998**, *451*, 163.
44. Salavagione, H.J.; Arias-Pardilla, J.; Perez, J.M.; Vazquez, J.L.; Morallon, E.; Miras, M.C.; Barbero, C.; *J. Electroanal. Chem.* **2005**, *576*, 139.
45. Carreño A.; Gacitúa M.; Valenzuela N.; Manríquez J.M.; Vega A.; Chávez I.; *Resumos da 8th Workshop in Computational Chemistry and Molecular Spectroscopy*, Punta de Tralca, Chile, 2012.
46. Carreño A.; Preite M.; Manríquez J.M.; Chávez I.; Vega A.; *Resumos da 2nd International Conference on Materials Science*, Valdivia, Chile, 2013.

SYNTHESIS, CHARACTERIZATION AND COMPUTATIONAL STUDIES OF (E)-2-[[2-(AMINOPYRIDIN-3-YL)IMINO]-METHYL]-4,6-DI-TERT-BUTYLPHENOL

Alexander Carreño^a, Andrés Vega^{a,†}, Ximena Zarate^b, Eduardo Schott^b, Manuel Gacitúa^c, Ninnette Valenzuela^c, Marcelo Preite^d, Juan M. Manríquez^c and Ivonne Chávez^{c,*}

^aDepartamento de Ciencias Químicas, Facultad de Ciencias Exactas, Universidad Andrés Bello, República 275, Santiago, Chile

^bLaboratorio de Bionanotecnología, Departamento de Ciencias Químico-Biológicas, Universidad Bernardo O'Higgins, General Gana 1780, Santiago, Chile

^cDepartamento de Química Inorgánica, Facultad de Química, Pontificia Universidad Católica de Chile, Avenida Vicuña Mackenna 4860, Santiago, Chile

^dDepartamento de Química Orgánica, Facultad de Química, Pontificia Universidad Católica de Chile, Avenida Vicuña Mackenna 4860, Santiago, Chile

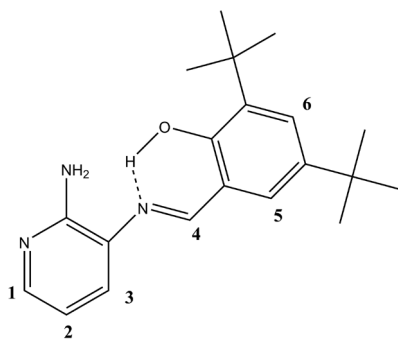


Figure 1S. Numbering of protons used in the ¹H NMR study of compound 3

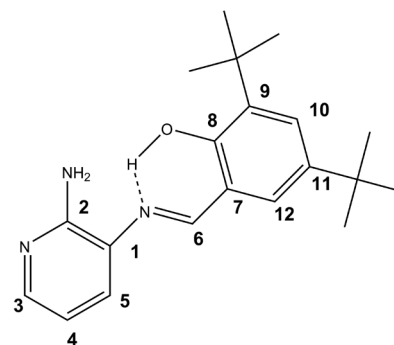


Figure 2S. Numbering of carbons used in the ¹³C NMR study of compound 3

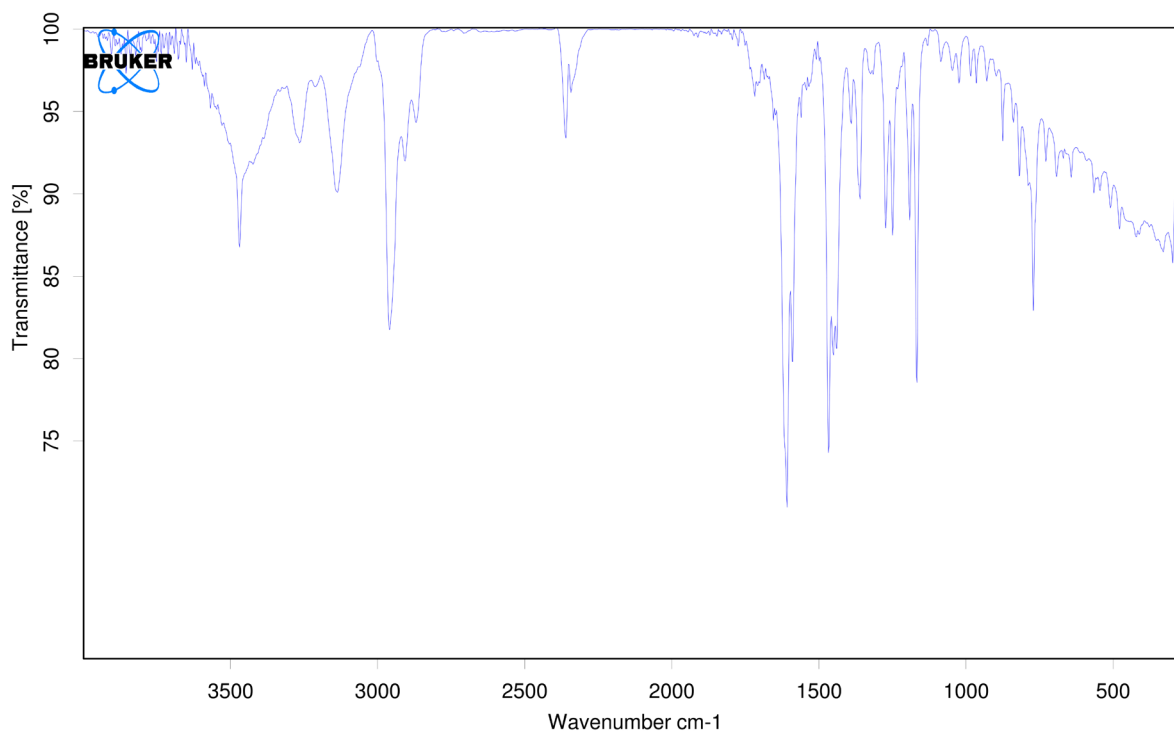


Figure 3S. FT-IR spectra of compound 3

*e-mail: ichavez@uc.cl

[†]Centro para el Desarrollo de la Nanociencia y la Nanotecnología, CEDENNA

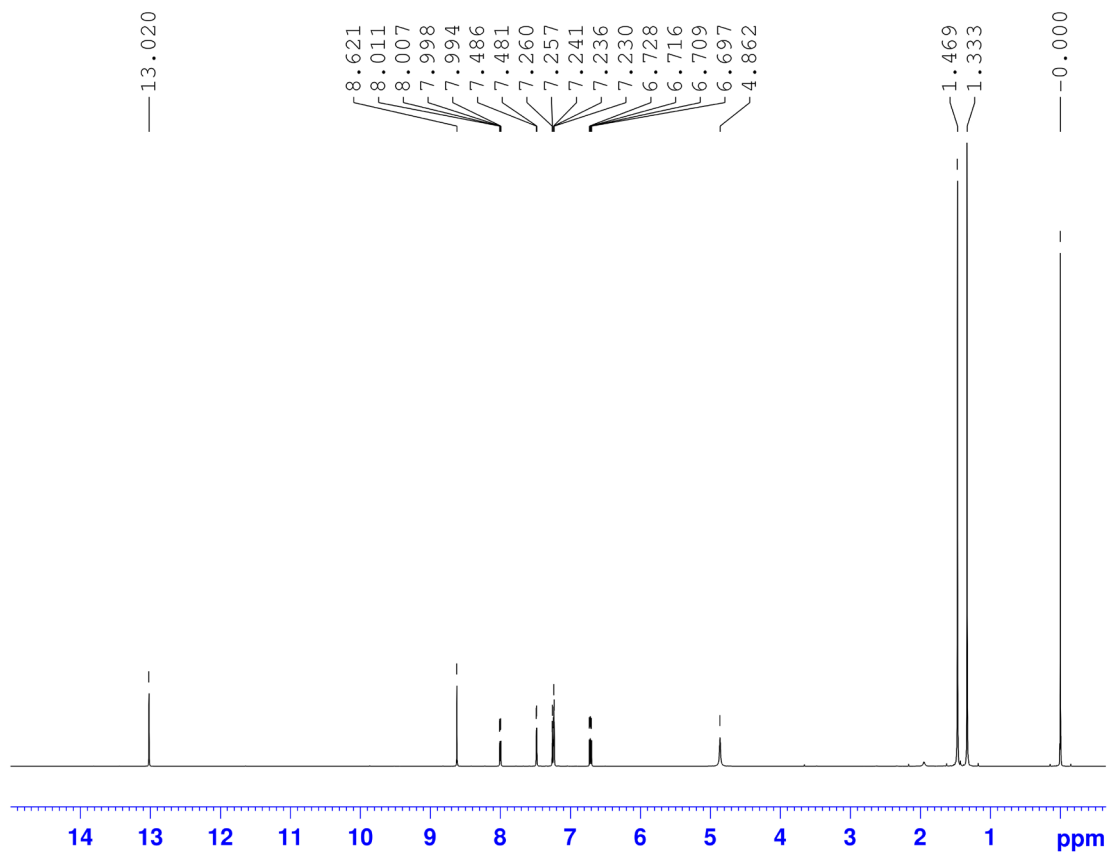


Figure 4S. ^1H NMR spectra of compound 3 in CD_3Cl

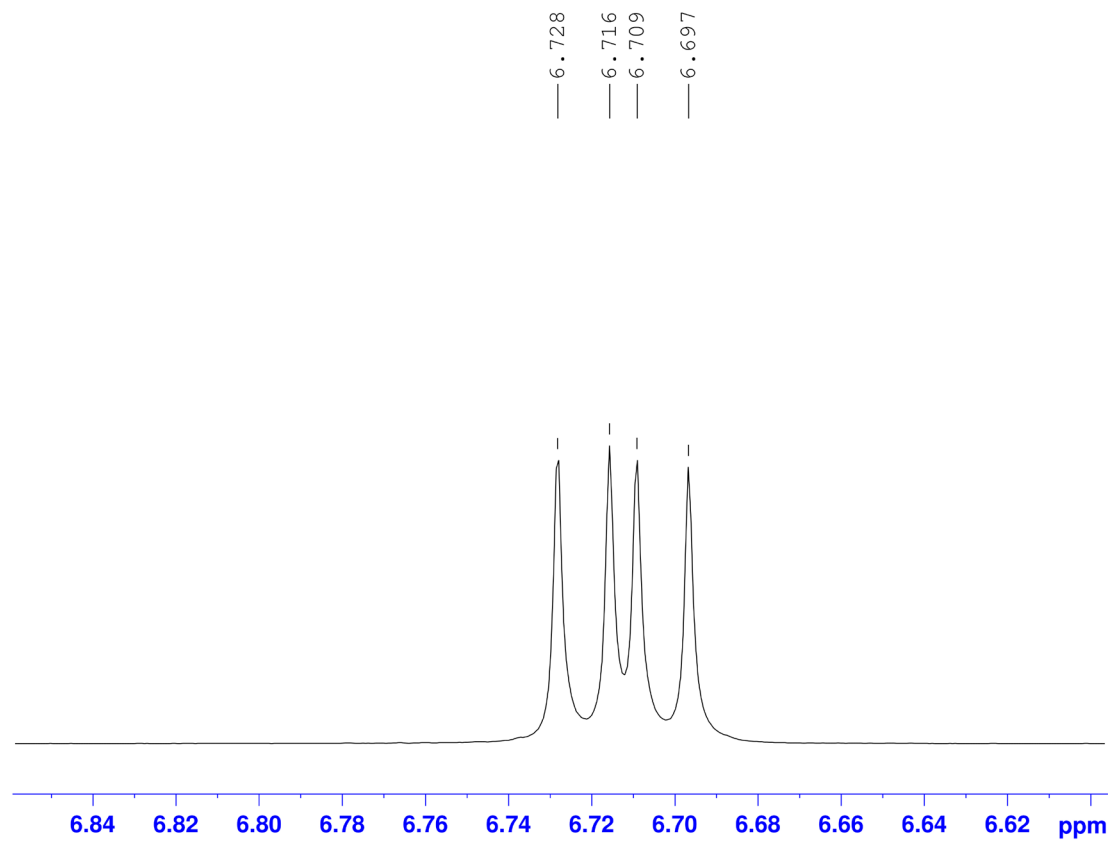


Figure 5S. Aromatic expanded regions of ^1H NMR spectra for H2 of compound 3 in CD_3Cl

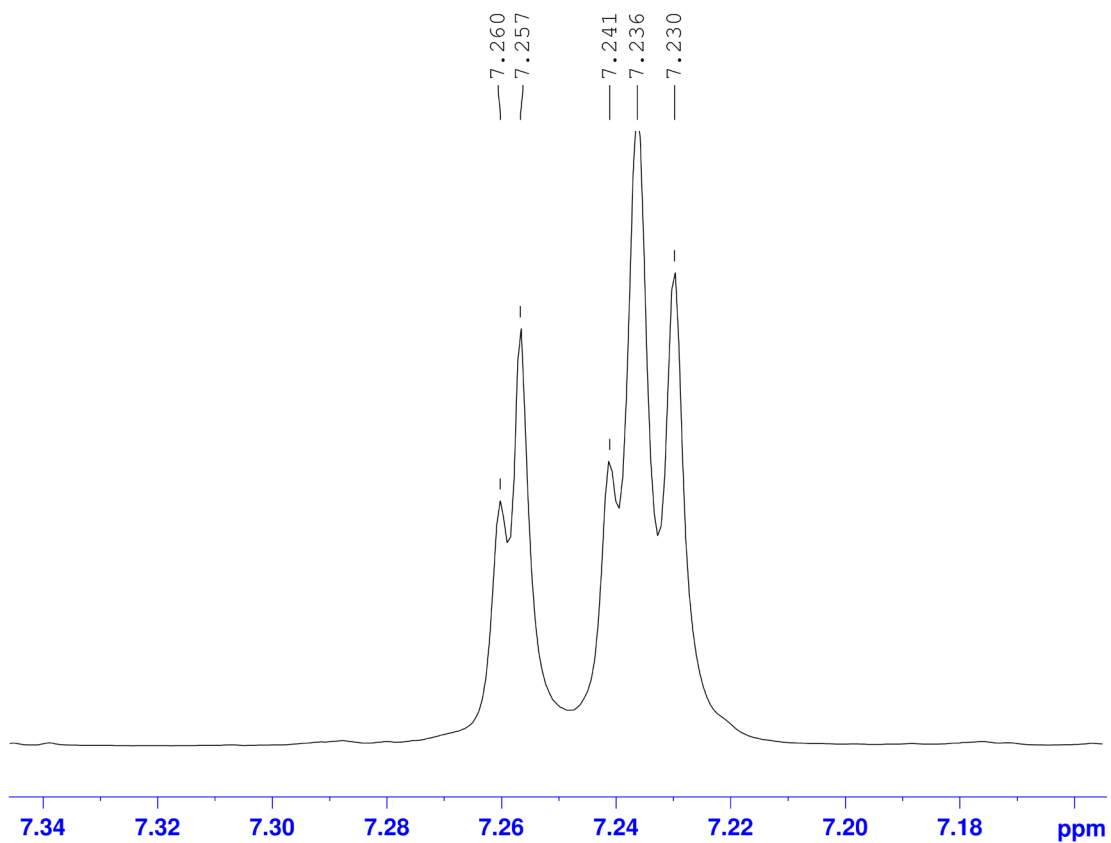


Figure 6S. Aromatic expanded regions of ^1H NMR spectra for H5 and H3 of compound 3 in CD_3Cl

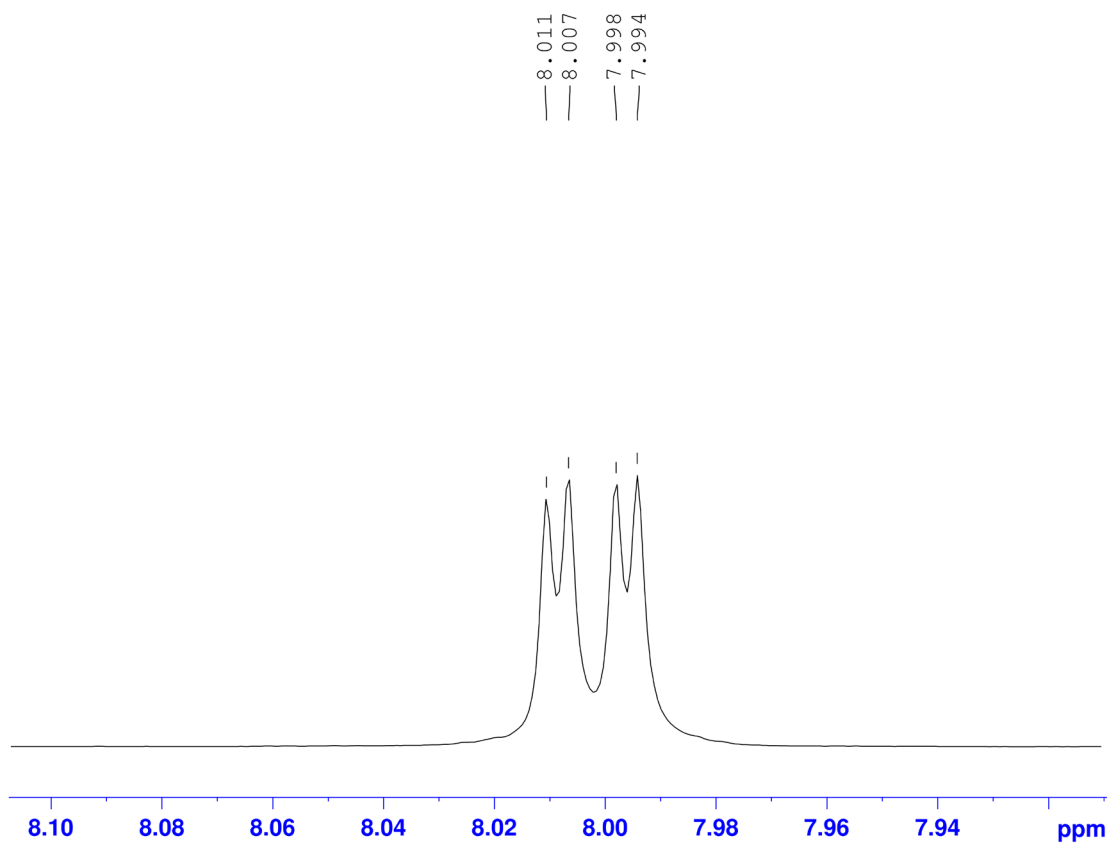


Figure 7S. Aromatic expanded regions of ^1H NMR spectra for H1 of compound 3 in CD_3Cl

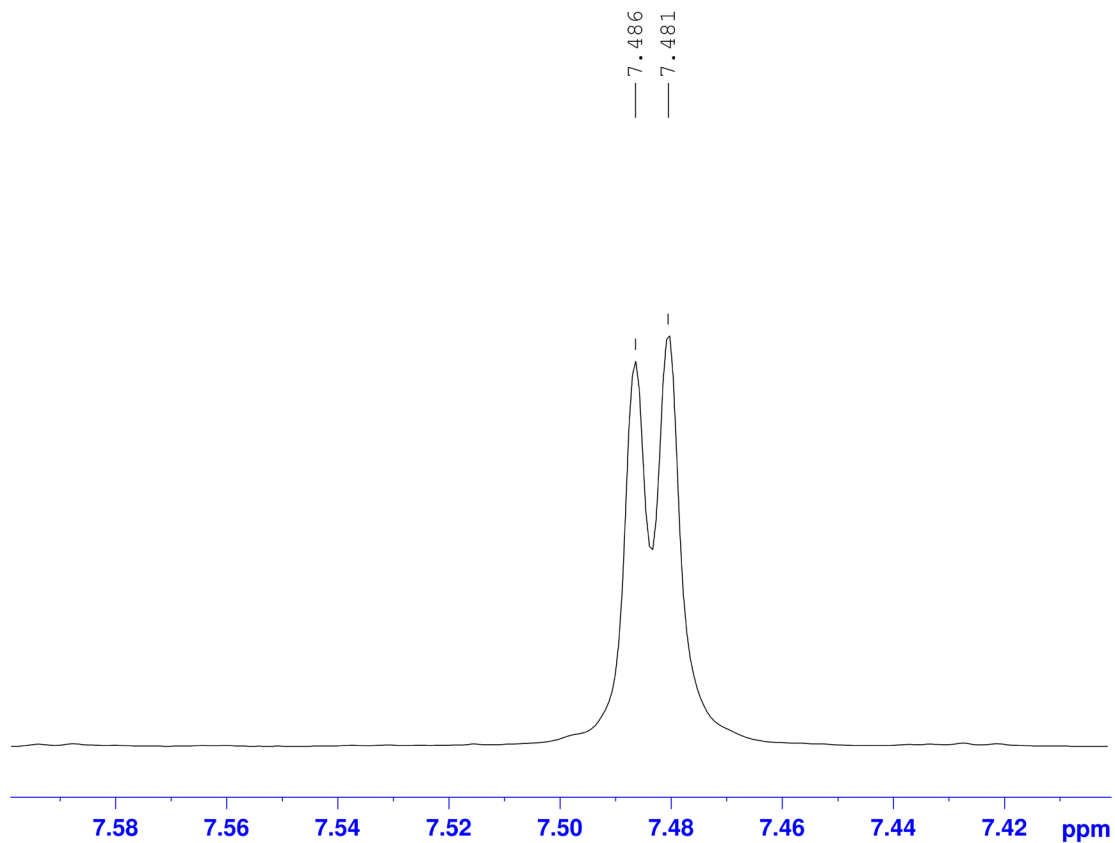


Figure 8S. Aromatic expanded regions of ^1H NMR spectra for H6 of compound 3 in CD_3Cl

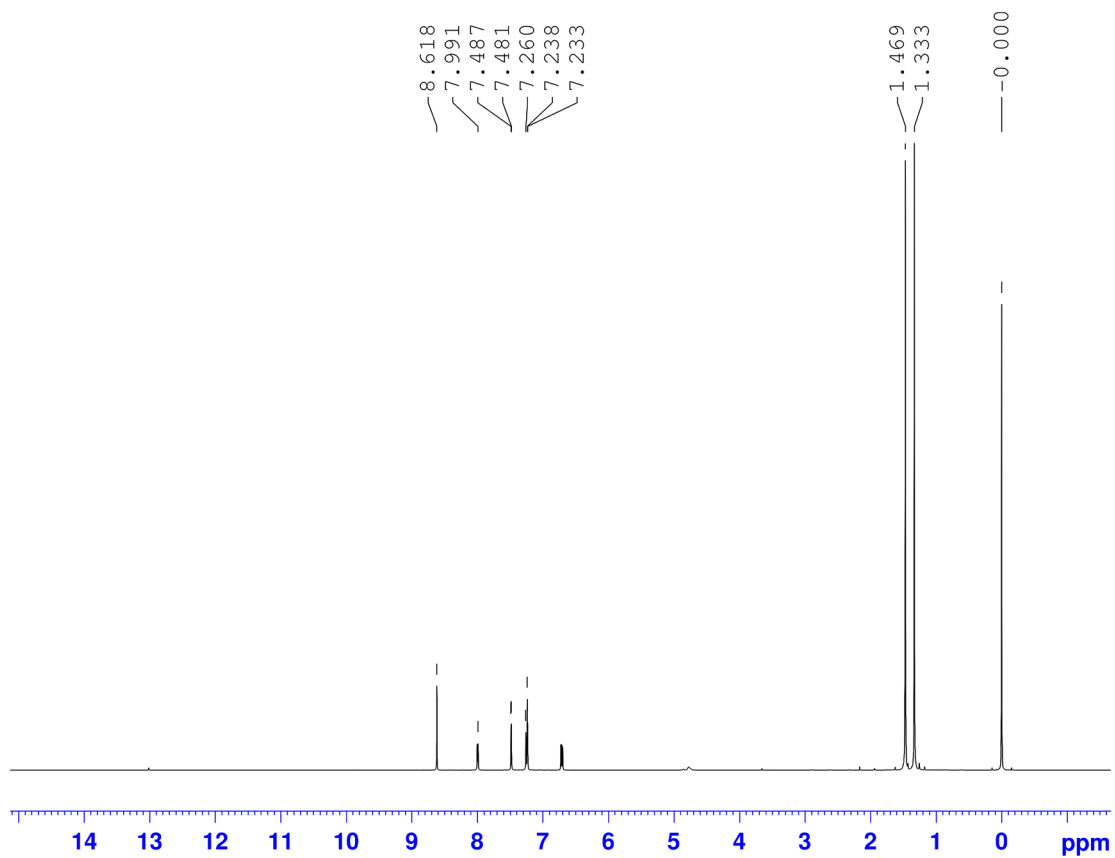


Figure 9S. D_2O exchange ^1H NMR spectra of compound 3 in CD_3Cl

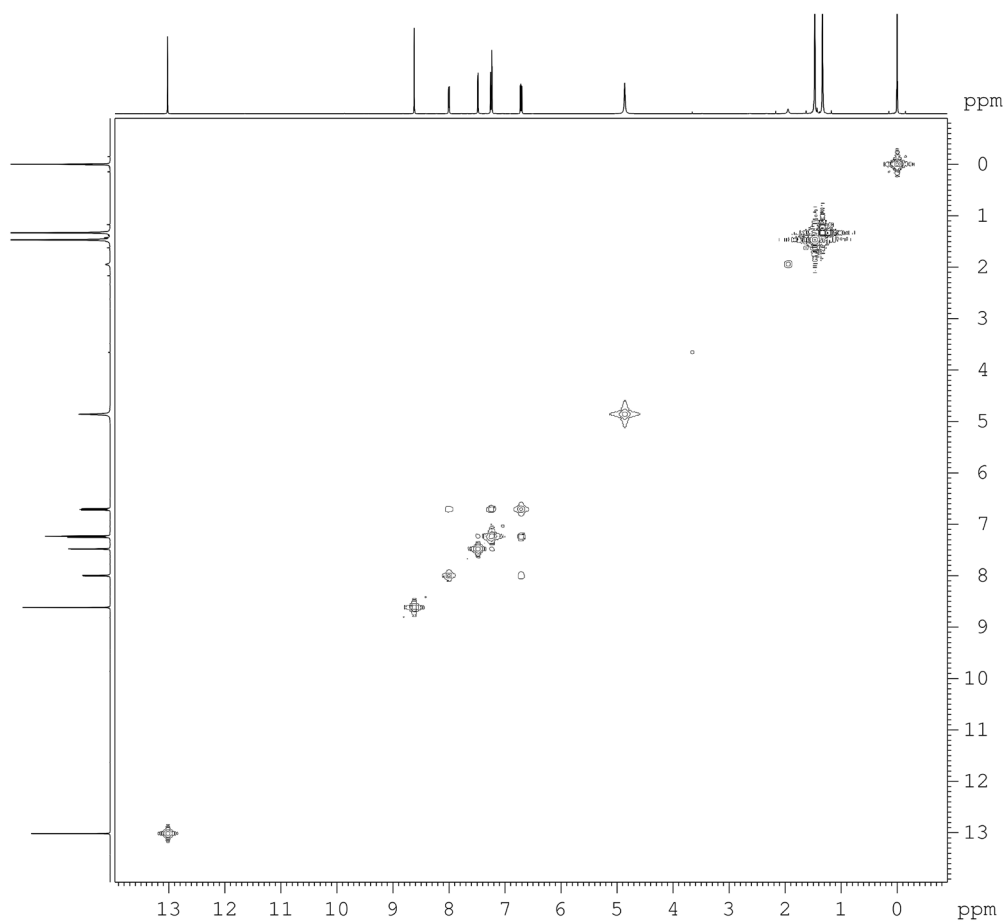


Figure 10S. HHCOSY spectra of compound 3 in CD_3Cl

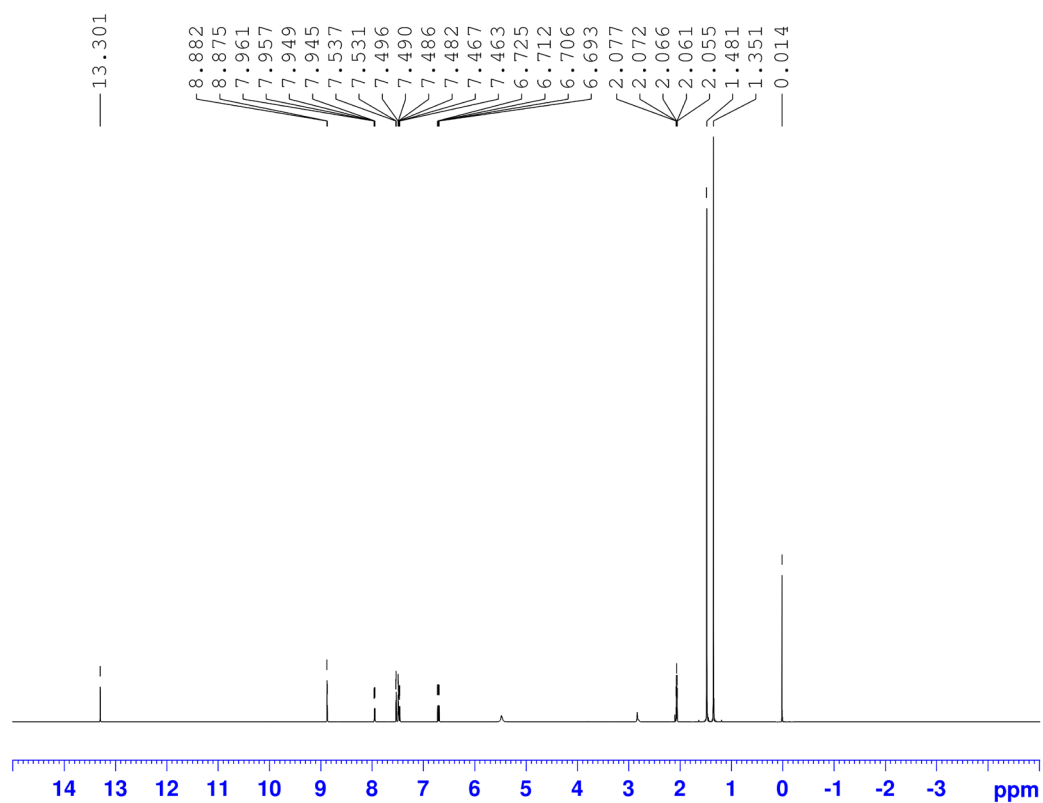


Figure 11S. 1H NMR spectra of compound 3 in $acetone-d_6$

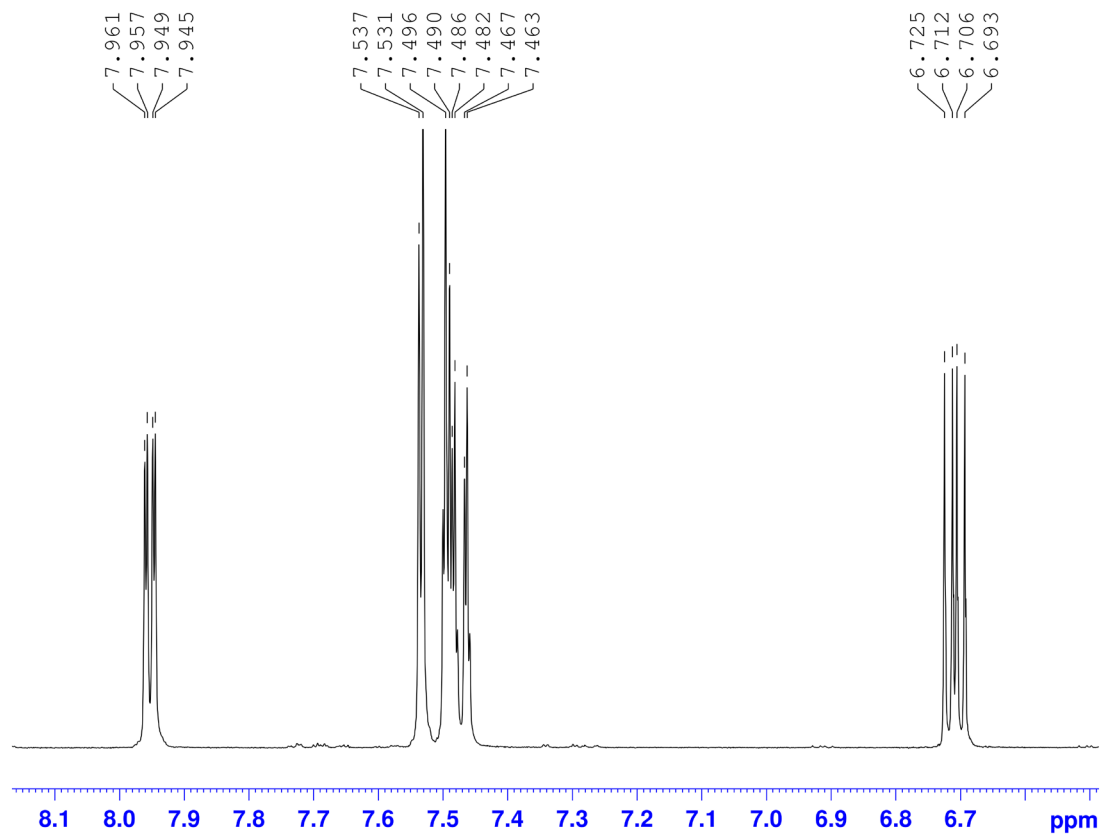


Figure 12S. Aromatic expanded regions of ^1H NMR spectra of compound 3 in acetone-d_6

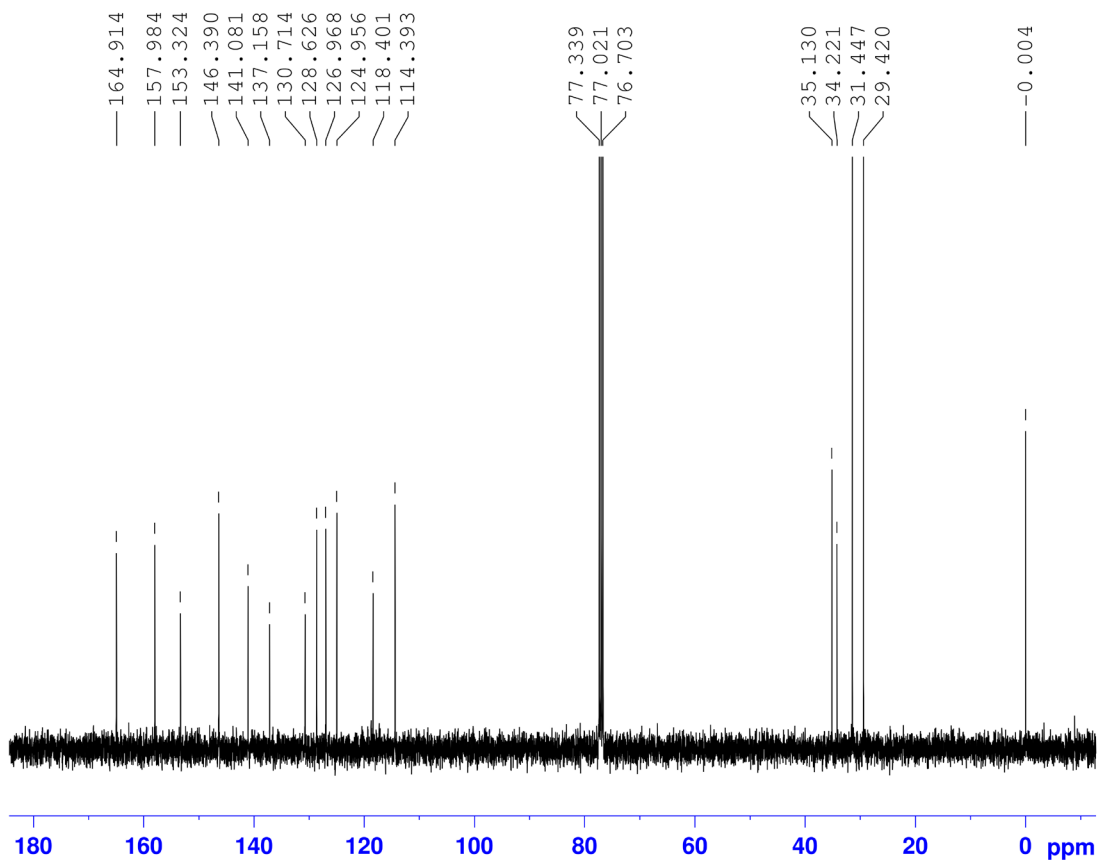


Figure 13S. ^{13}C NMR spectra of compound 3 in CD_3Cl

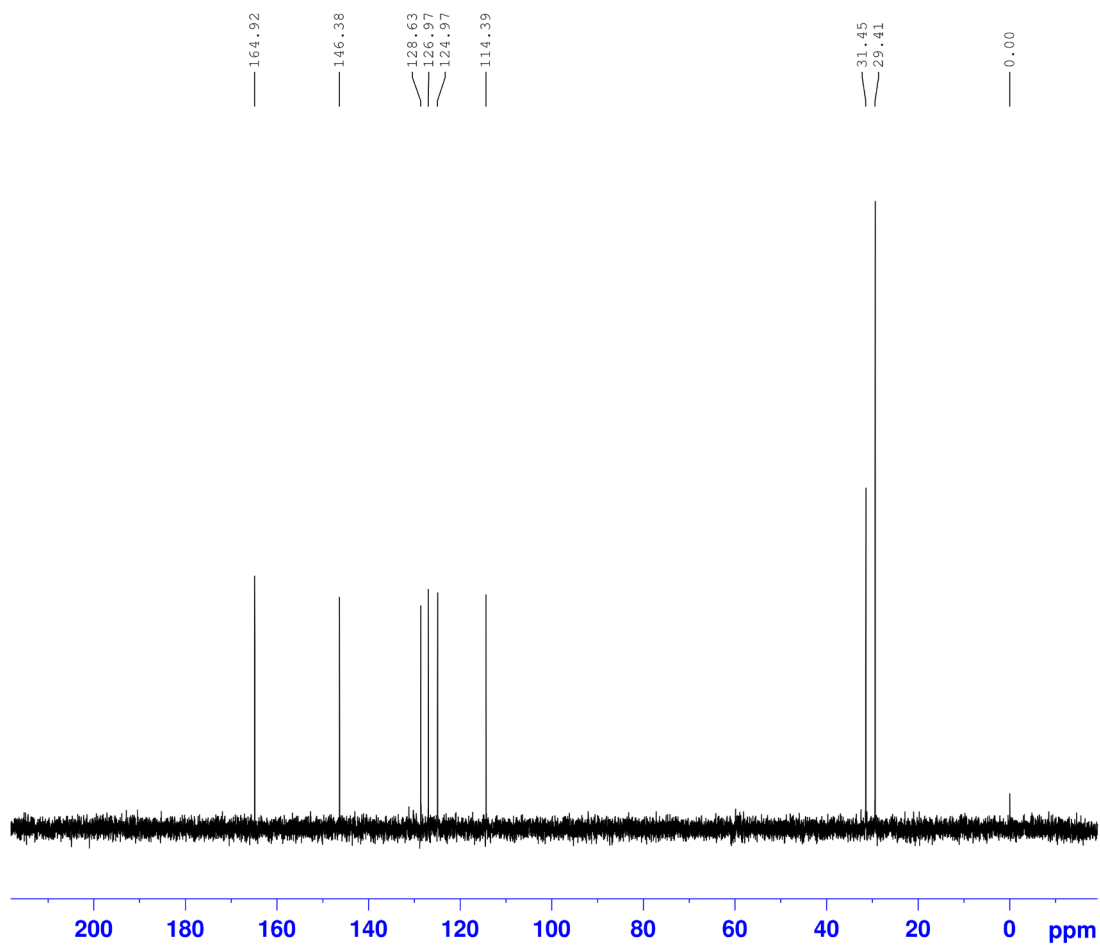


Figure 14S. DEPT spectra of compound 3 in CD₃Cl